Available online at www.sciencedirect.com
ScienceDirect
Journal of the European Ceramic Society 26 (2006) 3861–3870
www.elsevier.com/locate/jeurceramsoc

Effects of TiC/TiN addition on the microstructure and mechanical properties of ultra-fine grade Ti (C, N)–Ni cermets

Ning Liu *, Sheng Chao, Xinming Huang

Department of Materials Science and Engineering, Hefei University of Technology, Hefei 230009, PR China

Received 22 August 2005; received in revised form 26 October 2005; accepted 3 December 2005
Available online 14 February 2006

Abstract

Two series of Ti (C, N)-based cermets, one with TiC addition and the other with TiN addition, were fabricated by conventional powder metallurgy technique. The initial powder particle size of the main hard phase components (Ti (C, N), TiC and TiN) was nano/submicron-sized, in order to achieve an ultra-fine grade final microstructure. The TiC and TiN addition can improve the mechanical properties of Ti (C, N)-based cermets to some degree. Ultra-fine grade Ti (C, N)-based cermets present a typical core/rim (black core and grayish rim) as well as a new kind of bright core and grayish rim structure. The average metallic constituent of this bright core is determined to be 62 at% Ti, 25 at% Mo, and 13 at% W by SEM–EDX. The bright core structure is believed to be formed during the solid state sintering stage, as extremely small Ti (C, N)/TiC/TiN particles are completely consumed by surrounding large WC and Mo_2C particles. Low carbon activity in the binder phase will result in the formation $(Ni_2Mo_2W)C_x$ intermetallic phase, and the presence of this phase plays a very important role in determining the mechanical properties of TiN addition cermets.

Keywords: Mechanical properties; TiC; TiN

1. Introduction

The unique combination of mechanical properties such as excellent wear resistance and good chemical stability at elevated temperature makes titanium carbonitride based (Ti (C, N)-based) cermets be of great importance in metal cutting operations.[1] Nowadays, cermet cutting tools are widely used for semi-finishing and finishing works on steel and cast iron.[2] Since the introduction of nitrogen into TiC–Ni–Mo cermet systems as early as 1970s, the cutting performance of cermet materials has been significantly improved as a result of refined microstructure especially the grain size of hard phase.[3] Modern cermets normally consist of TiC + TiN/TiC_xN_{1-x} as main hard components and Ni/Co/Ni + Co as metal binder which bonds the carbonitride ceramic phase. In addition, 20–40 mass fraction of Mo_2C, WC, TaC, NbC and VC are usually added to improve the sinterability, hot hardness and thermal shock resistance.[4,5]

Comparing with conventional WC–Co cemented carbide, the microstructure of Ti (C, N)-based cermets is far more complicated, which is greatly influenced by the starting powder composition, particle size, particle size distribution as well as the sintering atmosphere. Normally, hard particles (carbonitride grains) exhibit a well-known core/rim structure. The core is essentially undissolved Ti (C, N) initial powder and the rim is enriched in heavier elements such as W, Mo, Ta, Nb which also has a cubic crystal structure. This core/rim structure has been studied by many authors and is widely believed to be the result of a dissolution–reprecipitation process.[6–8]

Previous works have shown that nano grain-sized WC–Co cemented carbides present quite different microstructure and mechanical properties as compared with conventional coarse-grained materials.[9,10]. In addition, it was reported that nano-sized TiN addition is more effective than micron-sized TiN addition in improving the mechanical properties of TiC-based cermets.[11] However, hitherto, there are few reports on the study of ultra-fine grade Ti (C, N)-based cermets.[12] This study aims to investigate the microstructure of Ti (C, N)-based cermets fabricated from nano/submicron-sized powders and related it to their mechanical properties. Special emphasis is paid on the study of

* Corresponding author. Tel.: +86 551 2901362; fax: +86 551 2905383.
E-mail address: ningliu@mail.hf.ah.cn (N. Liu).

0955-2219/$ – see front matter © 2005 Elsevier Ltd. All rights reserved.
doi:10.1016/j.jeurceramsoc.2005.12.010

Table 1
Main characteristics of the starting powders

Powder	Particle size (μm)	Chemical composition (wt.%)
TiC	0.33[a]	C_{free} < 0.5, Cl < 0.25, O<1.0
TiN	0.07[a]	C < 1.0, O < 2.0
Ti ($C_{0.5}$ $N_{0.5}$)	0.12[a]	C_{free} < 0.5, Cl < 0.25, O < 1.0
WC	1.14 (Fsss)	C_{free}: 0.02
Mo	2.33 (Fsss)	C: 0.0036, Fe: 0.002, O :0.095
Ni	2.95 (Fsss)	C < 0.15, S < 0.001, O < 0.015, Fe < 0.01
Carbon black	3.25 (Fsss)	N: 0.00015, O: 0.3

Fsss: fisher sub-sive size.
[a] From SEM/TEM analysis, other values come from datasheets of the producers.

Table 2
Nominal composition of cermets samples (in wt.%)

Cermets	Ti (C, N)	TiC	TiN	WC	Mo	Ni	C
A	49	0	0	15	15	20	1
B1	46.5	2.5	0	15	15	20	1
B2	44	5	0	15	15	20	1
B3	41.5	7.5	0	15	15	20	1
B4	39	10	0	15	15	20	1
C1	46.5	0	2.5	15	15	20	1
C2	44	0	5	15	15	20	1
C3	41.5	0	7.5	15	15	20	1
C4	39	0	10	15	15	20	1

how different TiC/Ti (C, N) and TiN/Ti (C, N) ratio influences the cermets' final microstructure and mechanical properties.

2. Experimental procedure

2.1. Materials processing

Some characteristics of the commercial powders are listed in Table 1. The particle morphology of main hard components (Ti ($C_{0.5}N_{0.5}$) abbreviated as Ti (C, N) afterward, TiC, TiN) was observed by SEM as shown in Fig. 1. Totally nine different starting compositions are designed, and their nominal compositions are given in Table 2.

All cermets samples were fabricated by the same conventional powder metallurgy method. Firstly, powders were weighted and dispersed in an ultrasonic cleaner for 30 min using ethanol as dispersant. Then they were milled with WC–Co balls (ball-to-powder weight ratio: 8/1) in ethanol bath by a planetary ball mill for 36 h. After milling, the slurry mixture was dried for 12 h at the temperature of 80 °C, and then sieved through 200 mesh and pelletised with 8% wax in a ceramic pot for an hour. Green compacts were prepared by pressing at the uniaxial pressure of 200 MPa, and dewaxed in the range 200–800 °C. Finally, vacuum sintering (0.1 Pa) was conducted at 1440 °C for an hour. Fig. 2 presents the sintering procedure curve.

2.2. Experimental methods

The microstructure of polished specimens (finished with 1 μm diamond paste) was observed by SEM (LEO-1530VP, LEO, Germany) in back-scattered-electron (BSE) mode coupled with EDX (OXFORD INCA X-Sight, UK), and the morphology of fractured surface was observed in secondary electron (SE) mode. In this study only metallic constitutes of each sample were measured since carbon and nitrogen content cannot be accurately quantified from SEM–EDX. Phase identification of each system was determined by XRD (D/max-rB, Rigaku, Japan) and the lattice parameter of crystalline phase was calculated by using Nelson-Riley function[13] (Ni-filtered Cu Kα

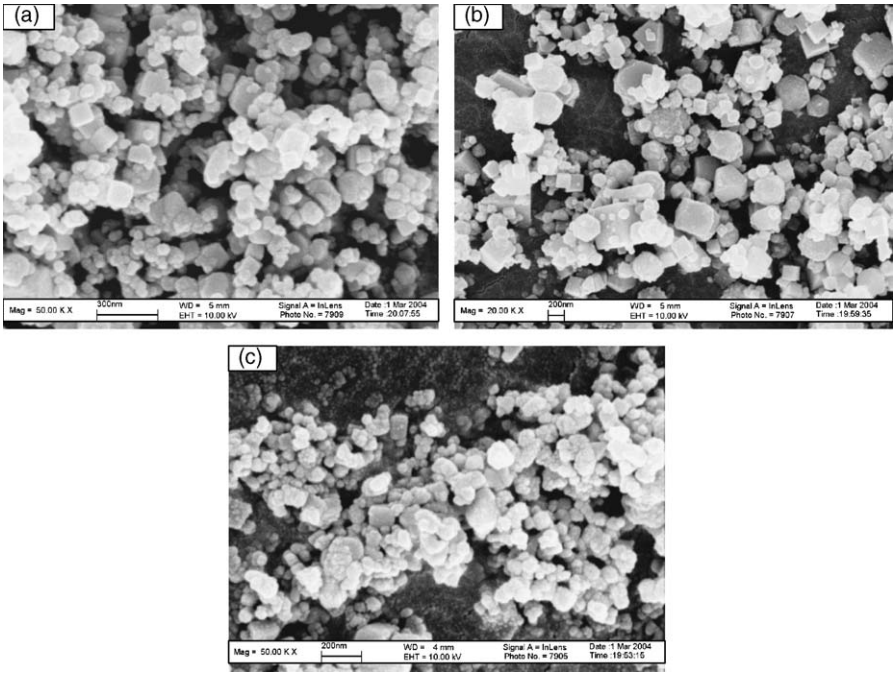

Fig. 1. SEM micrographs of main hard phase powders: (a) Ti (C, N); (b) TiC; (c) TiN.

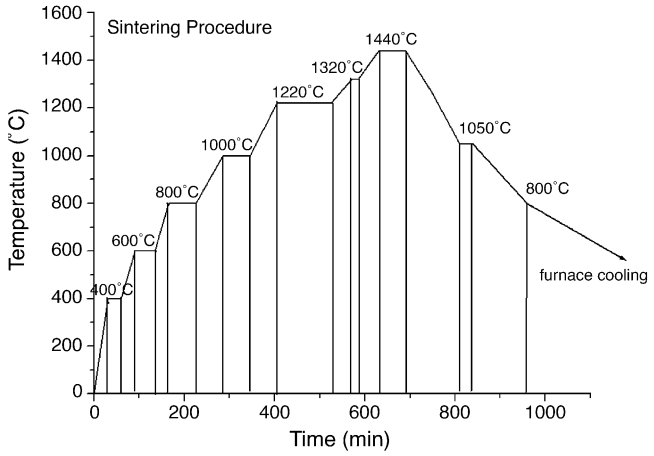

Fig. 2. The sintering procedure curve.

radiation, $85° < 2\theta < 145°$ angular ranger, 0.02° angle step). Three-point-bending transverse rupture strength (TRS) (20 mm span, 0.5 mm/min crosshead speed) and fracture toughness (K_{IC}) (Single Edge Notched Beam, SENB method) test was carried out on a Shimadzu DCS-5000 Universal Testing Machine (Japan) at room temperature. The specimen geometric sizes are 5 mm × 5 mm × 30 mm and 2.5 mm × 5 mm × 30 mm for TRS and K_{IC} testing, respectively. Vickers indentation hardness measurement was conducted under the condition of 10 kg load, 15 s loading time.

3. Results and discussion

3.1. As sintered materials

Representative SEM–BSE micrographs of each sample system are presented in Fig. 3. It shows that all specimens contain cores which give a dark BSE contrast, suggesting that their average atomic weight is lighter than the other parts. SEM–EDX analysis reveals that Ti is the dominant metallic constituent (>95 at%) of these dark cores, with little amount of Mo and W. The grayish rim surrounding the dark core shares the same metallic elements as core, but the content of Mo and W is much higher. Those intergranular-shaped regions that give a bright BSE contrast are Ni-based binder phases, in which Ti, Mo and W were also detected.

In addition to the above described Ti (C, N)-based cermets' common features, a distinctive microstructural feature is found in these ultra-fine grade cermets. A new kind of bright core and grayish rim structure can be easily identified from all of the nine sample systems. Seen from Fig. 3a, the BSE contrast of bright core is similar to that of the binder phase, indicating the existence of heavier elements when compared with dark cores.

3.2. Microstructure and phase composition

From Fig. 3, it can be seen that with the increasing amount of TiC addition (see Fig. 3b–e), more of the relatively coarser (comparing with finer Ti (C, N)) TiC particles were preserved in the microstructure as large dark cores. On the contrary, the microstructure of cermets C1–C4 (see Fig. 3f–i) becomes finer with increasing TiN addition. On one hand, this can be attributed to nano-sized initial TiN particles which may be still preserved in the final microstructure. On the other hand, the TiN addition effectively refrains the grain growth. It is a well-known that the grain growth rate in nitrogen-containing cermets is much lower than in nitrogen-free cermets, because the solubility of TiC in liquid Ni is significantly higher than that of TiN.[1] As a result, the grain growth (i.e. rim thickness) is repressed, as less substance is available to reprecipitate as rim phase.

Detailed results of EDX analysis of each phase (labeled as DC, BC, GR and B in Fig. 3a) are shown in Table 3. And their typical EDX spectrums are presented in Fig. 4. Previous studies have confirmed that those dark cores are remnants of the starting Ti (C, N) powders,[14] with little amount of Mo and W that may come through dislocations and other crystal defects.[15] Onto these cores, a Mo, W-rich rim phase grows through a dissolution and reprecipitation process. That is to say, partially dissolved Ti (C, N) together with completely dissolved WC and Mo_2C (during the sintering stage, molybdenum reacts with carbon to form Mo_2C) reprecipitates from binder phase and grows using those remaining Ti (C, N) cores as nucleation sites. Usually an inner rim structure is at the interface of the dark core and grayish outer rim in micron cermets' microstructure, with a Mo and W content even higher than the outer rim.[4,16,17] Interestingly, however, this inner rim structure is hard to be found in ultra-fine grade cermets of this study. Instead, a new kind of bright core exists, holding a metallic constituent close to reported inner rim composition.

The raw materials used in this study are Ti (C, N), TiC, TiN, WC and Mo, not (Ti, Mo, W) (C, N) pre-alloyed carbonitrides. Therefore (Ti, Mo, W) (C, N) bright cores must be formed during the sintering stage. The exact formation mechanism of this kind of core/rim structure is still unknown, but could be reasonably speculated. Commonly observed inner rim structure is believed to be formed during solid state sintering as Mo and W that have dissolved in binder reprecipitates to form Mo and W enriched (Ti, Mo, W) (C, N) solid solution, because at this stage the nitrogen activity is low due to open porosity.[7,17,18] Considering that the metallic composition and concentration of bright core is similar to that of the inner rim, and the fact that they are also surrounded by grayish outer rims, formed during liquid phase sintering, the bright core should be formed before the appearance of grayish outer rim, i.e. during the solid state sintering.

Generally the grain size of bright cores is larger than dark Ti (C, N) core and they often cluster together, indicating that there are some local positions which favor the formation of this structure. The core-like morphology of (Ti, Mo, W) (C, N) solid solution (bright core) should be formed from powder particle's

Table 3
Average metallic constituent (at%) of each phase according to EDX analysis

Phase	Ti	Mo	W	Ni
Dark core	97	2	1	–
Bright core	62	25	13	–
Grayish rim	79	13	8	–
Binder	23	10	5	62

specific geometric configuration after mixing and compression. If some extremely small Ti (C, N)/TiC/TiN particles are fully embedded by larger WC and Mo_2C particles, there are good chances that they may be completely consumed to give a core rather than a rim morphology, because of short diffusion length. Fig. 5 presents a schematic drawing demonstrating the formation mechanism of bright core structure. Hence, in certain parts of the materials where Ti (C, N) core is absent (Ti, Mo, W) (C, N) solid solution core appears. Since there is no substantial compositional difference in different bright cores, its composition should be given by the thermodynamic equilibrium at the solid state sintering temperature. As the TiC addition increases, the

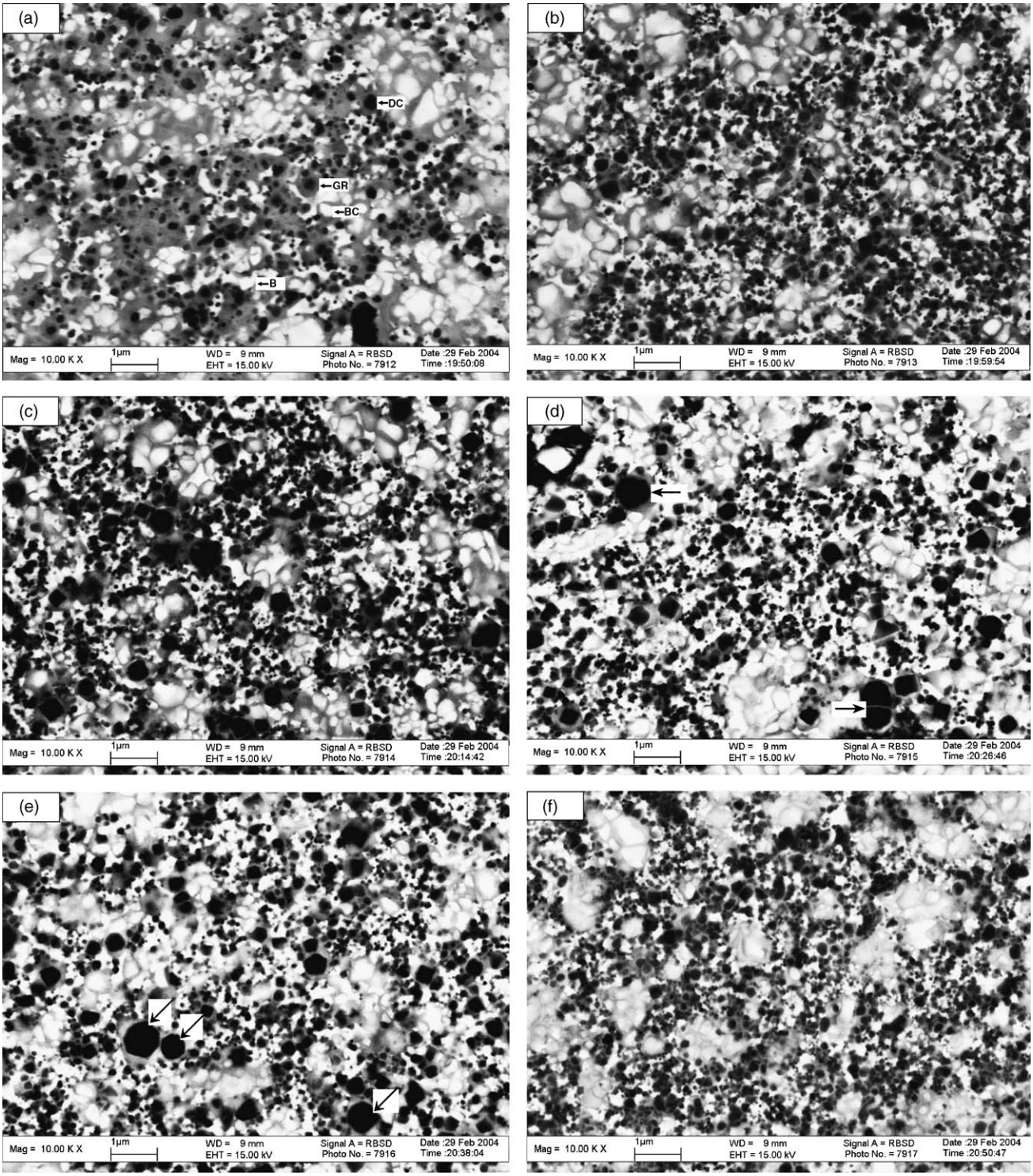

Fig. 3. SEM–BSE micrographs of each sample system: (a) cermet A; (b) cermet B1: (c) cermet B2; (d) cermet B3; (e) cermet B4; (f) cermet C1; (g) cermet C2; (h) cermet C3; (i) cermet C4 (DC stands for: dark core, BC stands for: bright core, GR stands for: grayish rim, B stands for: binder. Arrows indicate remaining big TiC cores in (d) and (e), and intermetallic phase $(Ni_2Mo_2W)C_x$ in (h) and (i)).

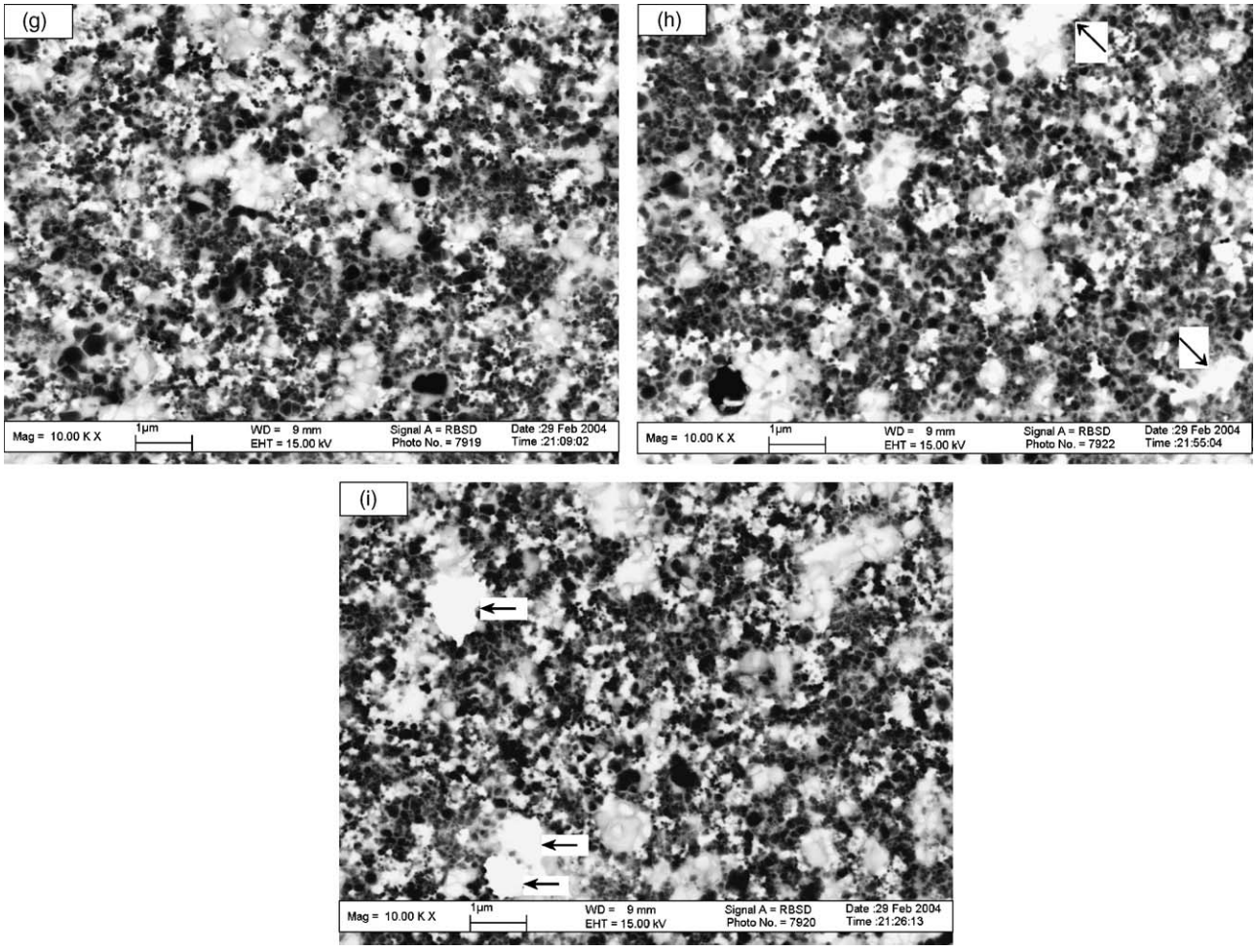

Fig. 3. (*Continued*)

volume fraction of bright core structure has a trend to increases (see Fig. 3b–e). This is in agreement with literature,[14] which reported that a higher carbon activity will result in larger amounts of (Ti, W, Ta) (C, N) cores/inner rim structure.

In the case of TiN addition cermets, increasing the amount of TiN addition leads to the formation of a new phase which is indicated in Fig. 3h and i by arrows. The EDX result shows that the average composition of this phase is 40.1 at% Ni, 37.0 at% Mo, 19.4 at% W and 2.7 at% Ti, in addition C is also detected. Considering that little amount of Ti may derive from electron beam boarding effect, we can roughly denominate it as $(Ni_2Mo_2W)C_x$. The EDX spectrum of this phase is given in Fig. 6. The formation of this new phase should be related to the nitrogen or carbon activity in TiN addition cermets. Detailed discussion of this new phase is presented in the next section.

The Ni-based binder mainly distributes around the hard carbonitride grains. A lot of Ti, Mo and W are found in the binder phase which comes from dissolved WC and Mo_2C. Nevertheless, this composition does represent the equilibrium concentration of the metallic elements in the liquid Ni, because of too low diffusion rate and too short soaking time.

XRD pattern of some selected samples is shown in Fig. 6, from which it can be seen that Ti (C, N) phase exists in all sample systems while no WC and Mo_2C trace was detected, suggesting that they have fully dissolved into the carbonitride ceramic phase and Ni-based binder phase (considering the detection limit of XRD, small amount of WC and Mo_2C may still exist but their volume fraction should be less than 5%). This is in accordance with literature,[19] which reported that Mo reacts with carbon to form Mo_2C around the temperature of 1000 °C and then completely dissolves around 1200 °C. Similarly, WC dissolves a little bit slower which disappears form XRD pattern about 1300 °C.[19]

In the XRD patterns of cermets C3 and C4, peaks of above mentioned intermetallic phase $(Ni_2Mo_2W)C_x$ are observed as shown in Fig. 7. Since η phase presents in WC–Co hard mental and cermets in condition of carbon deficiency,[20] and it is reported that the dissolution of W and Ti in the binder phase can be controlled by total carbon content in cermets materials,[14] the presence of this intermetallic phase should be related to the carbon activity in cermets C3 and C4. As more TiN is added, more of it decomposes at high temperature and releases N_2 (TiN is subjected to thermal dissociation at high temperature[21]). This process is further promoted by the vacuum sintering atmosphere. Consequently, carbon atoms enter instead to refill the vacancy left by nitrogen. Therefore, less carbon black added is avail-

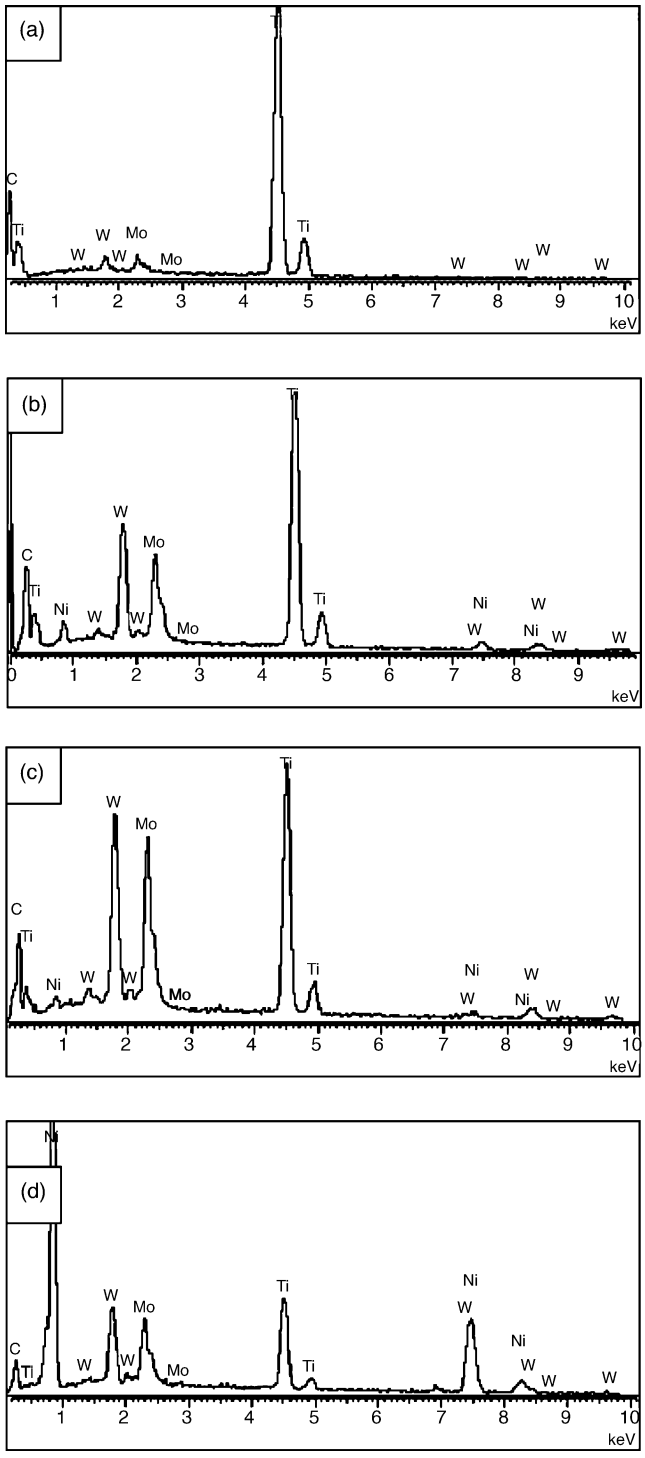

Fig. 4. Typical EDX spectrums of various phases: (a) dark Ti (CN) cores; (b) (Ti, Mo, W) (C, N) grayish rim; (c) (Ti, Mo, W)(C, N) bright core; (d) Ni-based binder.

able to maintain the cermets in the normal two phase areas. As a result, the solubility of Mo and W in the binder phase is substantially enhanced resulting from low carbon activity in the binder phase.

Peaks of Ti (C, N) and (Ti, Mo, W) (C, N) core/rim structures cannot be resolved at forward angular range ($30^\circ < 2\theta < 80^\circ$), because of their isomorphic crystal structure and very close lattice parameters. However, a careful XRD inspection scanned along the back-reflection angular range ($85^\circ < 2\theta < 145^\circ$) is able to discriminate them and calculate their small lattice parameter misfit. A typical XRD pattern carried out at back-reflection angular range is given in Fig. 8, from which it can be seen that carbonitride phase has split into two and even three peaks. The lattice parameters of (Ti, Mo, W) (CN) rim and (Ti, Mo, W) (C, N) cores as well as Ni based binder phase is listed in Table 4. These data indicate that the lattice parameter of (Ti, Mo, W) (C, N) bright core is slightly larger than that of outer rim phase for more Mo and W atoms dissolved into the Ti (C, N) lattice and randomly occupied the sublattice sites of Ti.[22] Since the ionic radius of Ti^{4+} is 0.68 Å which is smaller than W^{4+} 0.70 Å and

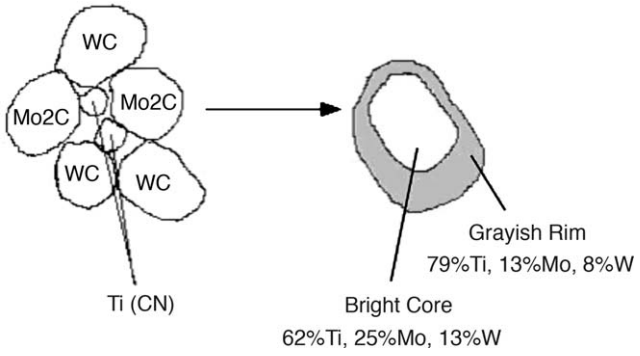

Fig. 5. Schematic drawing demonstrating the formation mechanism of bright core structure.

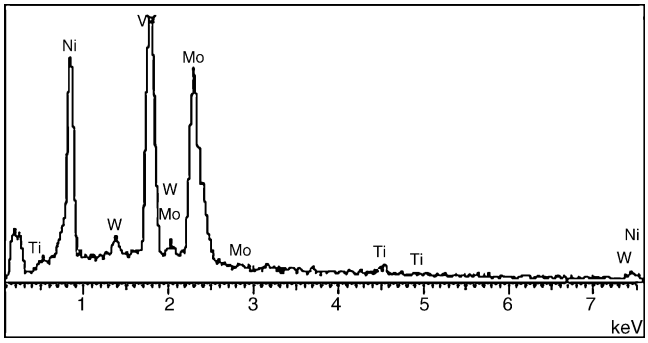

Fig. 6. EDX spectrum of the new phase found in cermets C3 and C4.

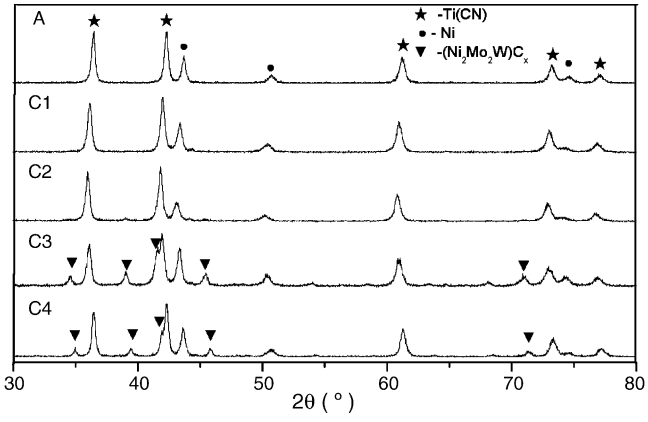

Fig. 7. XRD pattern of some selected cermet samples.

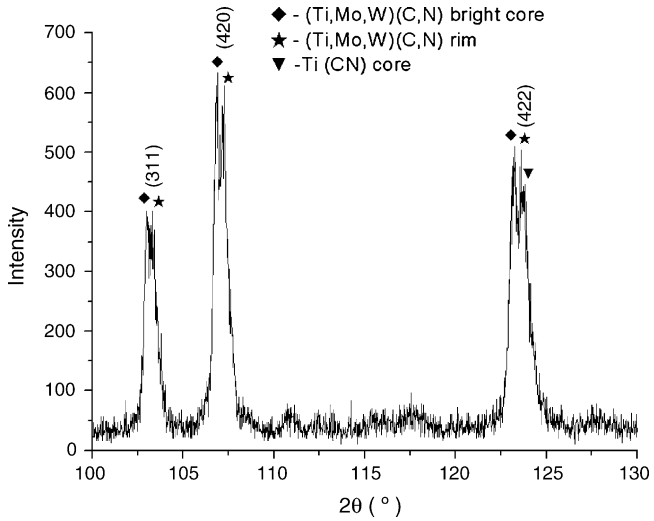

Fig. 8. XRD pattern of cermet C3 carried out at back-reflection angular range.

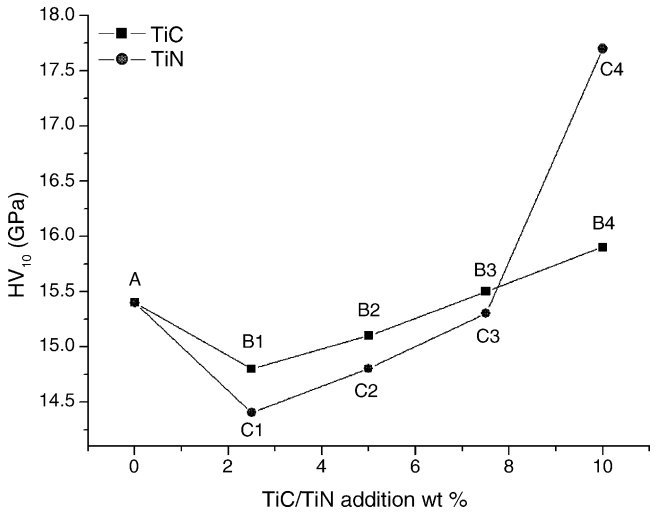

Fig. 9. TiC/TiN addition on the HV hardness.

Mo^{4+} 0.70 Å, the entrance of Mo and W atoms dilates the lattice parameter to some extent. The calculated misfit level with respect to the lattice parameter difference between (Ti, Mo, W) (C, N) rim and (Ti, Mo, W) (C, N) bright core is in the range of 0.21–0.33%, similar to the data found in literature.[23]

Considering that rim phase occupies a larger volume fraction than Ti (C, N) core phase, the left peaks of each double peak detected in back-reflection angular range should represent the rim structure more than the cores. And since the core is almost free of Mo and W, its lattice parameter must be smaller than that of rim. Hence, it could be said that the real lattice parameter misfit between dark core and bright core should be greater than the values mentioned above. If we use Ti (C, N) starting powder's lattice parameter to calculate the misfit level, this figure can be as large as 0.37%. However, it is still far below a critical value of 1.3% reported in literature,[18] in which the separation of inner rim phase from Ti (C, N) core was attributed to lattice mismatching, as misfit dislocation located at the core/rim interface approaches one another and finally leads to the physical separation of inner rim and core phase. According to their study,[18] the misfit level seems to be too small to cause the formation of the bright core structure. Thus, the formation of bright cores can be better explained as a result of promoted diffusional reaction, because of the extremely small powder particle size.

Table 4
Lattice parameter of various phases (nm)

Cermets	(Ti, Mo, W) (C, N) rim	(Ti, Mo, W) (C, N) core	Ni-based binder
A	0.4296	0.4310	0.3574
B4	–	–	0.3596
C1	–	–	0.3602
C2	0.4293	0.4304	0.3608
C3	0.4291	0.4306	0.3602
C4	0.4293	0.4302	0.3598
Ti (CN) starting powder	0.4290		
Standard Ni			0.3524

The lattice parameter of standard Ni is cited from JCPDS file 4-0850.

The XRD pattern clearly indicates that binder phase has a cubic crystal structure, with a lattice parameter that is substantially larger than pure Ni (see Table 4). This phenomenon suggests that considerable amount of Ti, Mo and W atoms have dissolved into Ni binder phase during the sintering stage, which corresponds well with the EDX results. The calculated lattice parameter of the binder phase in this study is on the whole larger than previous literature data,[23,24] which may be ascribed to the fact that both Mo and WC was added as starting materials instead of single addition of Mo or WC.

3.3. Mechanical properties

The mechanical property of cermets depends not only on their starting compositions but also on their microstructural features such as: grain size, grain size distribution, phase volume fraction and morphology, etc. The effects of TiC/TiN addition on Vickers hardness, transverse rupture strength and fracture toughness are shown in Figs. 9–11, respectively. It is denoted

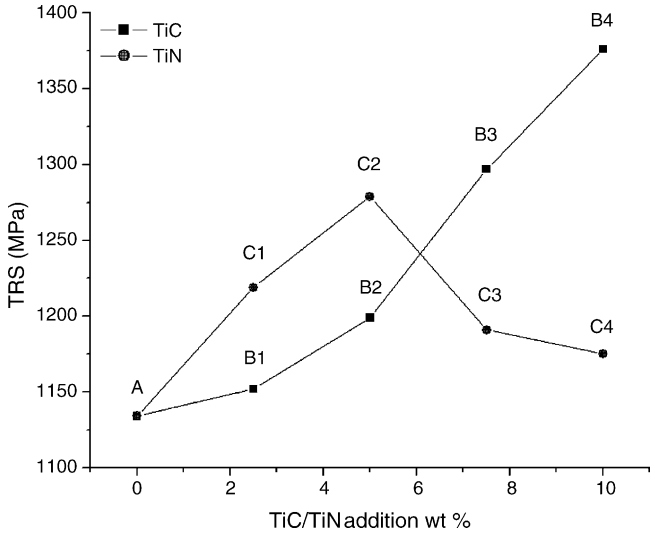

Fig. 10. TiC/TiN addition on the TRS.

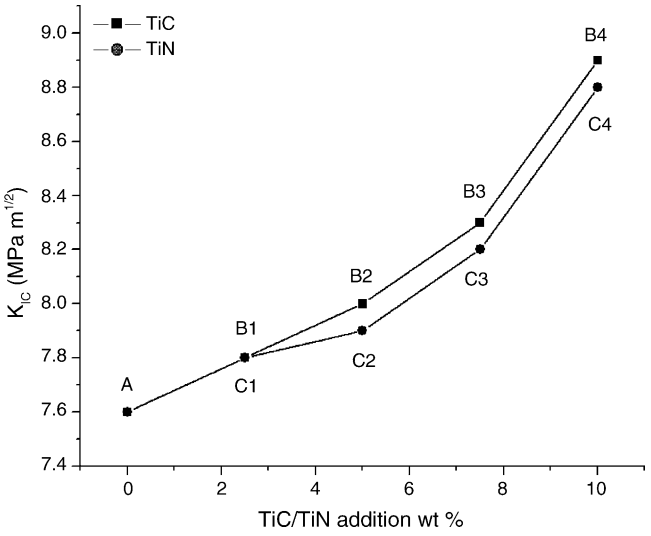

Fig. 11. TiC/TiN addition on the fracture toughness.

that with the increasing amount of TiC addition, Vickers hardness (HV_{10}) of cermets B1 to B4 goes up slowly. Since the micro hardness of TiC is much higher than TiN (TiC: 32 GPa, TiN: 20 GPa according to ref.[25]) the hardness values of all TiC-added cermets (B1 to B4) should be higher than cermets A, theoretically. However, this is not the case here. This phenomenon could be explained by their microstructure features. Seen from Fig. 3, the mean grain size of cermets B1 and B2 is larger than cermets A. So according to Hall–Petch formula, coarser grains in cermets B1 and B2 counteract the effect of small amount of TiC addition. Only when the TiC addition reaches the level of 7.5 wt.%, the hardness of cermets B3 and B4 begins to outreach cermets A.

The effect of TiN addition on the Vickers hardness is similar to TiC addition, except that hardness value increases significantly from cermets C3 to cermets C4. Since the TiN is softer than TiC as mentioned above, the hardness curve of cermets C1 to C3 is below that of cermets B1 to B3. But as TiN addition increases, the hardness difference between TiC addition cermets and TiN addition cermet has a trend to decrease, indicating that the Hall–Petch hardening effect becomes more and more evident as the addition of TiN increases. However, the greatly enhanced hardness value from cermets C3 to cermets C4 (16% of increase) should not be attributed to the finer microstructure alone. As discussed above, intermetallic phase $(Ni_2Mo_2W)C_x$ that is harder than Ni-base binder appears in cermets C3 and C4. Therefore, the highest hardness value achieved in cermet C4 should be mainly attributed to the presence of large amount of this phase. In fact, the hardness of cermets materials is not determined by ceramic phase alone, but follows a simple balance law just like WC–Co cemented carbides.[26] That is, various phases contribute to the hardness of bulk material, according to the hardness and volume fraction of each phase.

From Fig. 10, it can be seen that values increase as the amount of TiC addition increases up to 10 wt.%. However, when TiN is added, the TRS value reaches its highest value at 5.0 wt.% addition and then decreases.

From cermets B1 to cermets B4, the volume fraction of bright core and grayish rim structure tends to increase. Since those bright cores are not remaining Ti (C, N) particles but (Ti, Mo, W) (C, N) solid solution, and grayish rims are also composed of (Ti, Mo, W) (C, N), the distribution gradient of elements of this core/rim structure should be less than that of Ti (C, N) core and rim structure. Consequently, the interior stress induced from lattice parameter mismatch between core and rim at the interface of core/rim boundary is reduced too. Therefore, as more bright core and grayish rim structures appear in the final microstructure, the TRS value increases accordingly. This is consistent with previous study results.[27]

As the addition of TiN increases, the resulting microstructure becomes finer and finer. However, the TRS value does not go up monotonously, instead, there is a peak value occurring at 5.0 wt.% of TiN addition. This phenomenon can be attributed to two factors: (1) the presence of brittle-natured intermetallic phase $(Ni_2Mo_2W)C_x$, which may work as fracture initiator when it locates close to the load; (2) as more TiN decomposes, released N_2 leaves more residual porosity in the material, which reduces TRS value too. Combining these two factors, when TiN addition excesses 5.0 wt.%, the TRS value decreases immediately.

Micrographs of fractured surface of cermet B4 and cermet C4 are shown in Fig. 12a and b. It reveals that the typical fracture mode is intergranular fracture, however, transgranular fracture mode can be observed too, especially in relatively coarser ceramic grains. To cermets material, a strong core/rim and binder/rim bond is essential to bending strength improvement. Since good bonding usually occurs when the hard phase has a

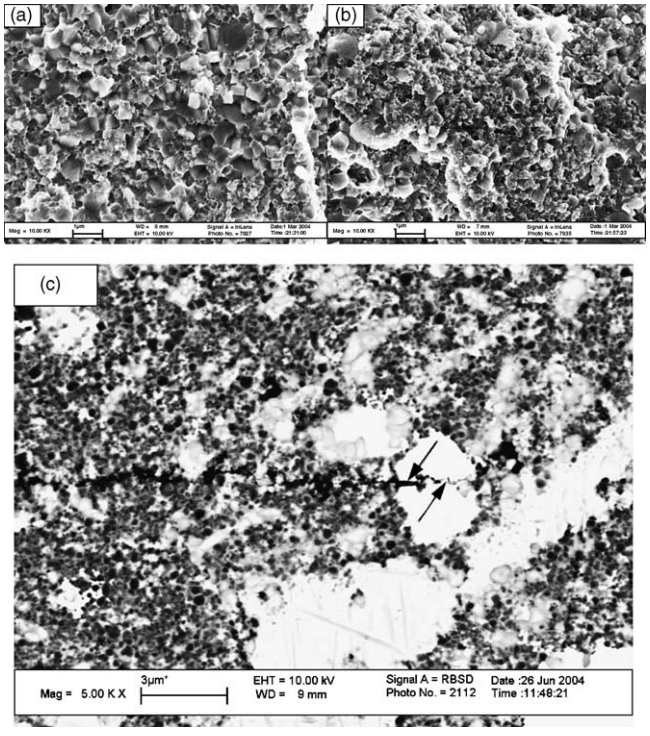

Fig. 12. Fractured surface of TRS testing samples: (a) cermets B4; (b) cermets C4; (c) crack propagating through the intermetallic phase.

limited solubility in the binder during liquid phase sintering,[28] inter-diffusion between core and rim as well as rim and binder is favored.

Both TiC and TiN addition improves the fracture toughness in a similar way as can be seen from Fig. 11. Fracture toughness is a kind of property that represents materials' resistance to crack propagation. As more TiC is added, more of them is preserved in the final microstructure as relatively coarser grains. And since generally cracks propagate along the grain boundaries in cermets materials, i.e. intergranular mode,[24] cermets with more coarser grains can more effectively deviate crack, resulting in more zigzagged crack propagation course and absorbing more energy correspondingly. Although the carbonitride grain size decreases as TiN addition increases, the K_{IC} value of cermet C1 to C4 increases too. Since the crack deflection mechanism mentioned above does not work here, there must be some other toughening mechanisms. Micropores resulting from the decomposition of TiN may toughen the TiN addition cermets to some extent. In addition, it was observed that cracks usually propagate through the intermetallic phase $(Ni_2Mo_2W)C_x$ (see Fig. 12c). Though $(Ni_2Mo_2W)C_x$ as a intermetallic phase could not as effectively as Ni binder in absorbing crack-tip energy by plastic deformation mechanism, it may still have some toughening effects because of its relatively larger size.[29] Therefore, the addition of TiN increases K_{IC} value steadily unlike the TRS which has a peak value.

4. Conclusions

In the present study, the microstructure and mechanical properties of TiC addition and TiN addition cermets were investigated. The conclusion of this study can be summarized as follows:

(1) Ultra-fine grade Ti (C, N)-based cermets present a typical core/rim (black core and grayish rim) as well as a new kind of bright core and grayish rim structure. The average metallic constitute of this bright core is determined to be 62 at% Ti, 25 at% Mo, and 13 at% W by SEM–EDX.
(2) The Bright core structure is believed to be formed during the solid state sintering stage, as extremely small Ti (C, N)/TiC/TiN particles are completely consumed by surrounding large WC and Mo_2C particles.
(3) Low carbon activity in the binder phase will result in the formation $(Ni_2Mo_2W)C_x$ intermetallic phase, and the presence of this phase plays a very important role in determining the mechanical properties of TiN addition cermets.
(4) In general, both the TiC and TiN addition can improve the mechanical properties of Ti (C, N)-based cermets to some degree; however, these improvements should be attributed to different mechanisms.

Acknowledgements

The authors wish to acknowledge the support of this research by the Natural Science Foundation of Anhui Province and the Natural Science Foundation of China under contract no. 03044902 and no.50072003, respectively.

References

1. Ettmayer, P., Kolaska, H., Lengauer, W. and Dreyer, K., Ti (C, N) cermets-metallurgy and properties. *Int. J. Refract. Met. Hard Mater.*, 1995, **13**, 343–351.
2. Pastor, H., Titanium-carbonitride-based hard alloys for cutting tools. *Mater. Sci. Eng. A*, 1998, **105/106**, 401–409.
3. Ettmayer, P., Kolaska, H. and Dreyer, K., Effect of the sintering atmosphere on the properties of cermets. *Powder Metall. Int.*, 1991, **23**(4), 224–229.
4. Chen, L., Lengauer, W. and Dreyer, K., Advances in modern nitrogen-containing hardmetals and cermets. *Int. J. Refract. Met. Hard Mater.*, 2000, **18**, 153–161.
5. Qi, F. and Kang, S., A study on microstructure changes in Ti (C, N)–NbC–Ni cermets. *Mater. Sci. Eng. A*, 1998, **251**, 276–285.
6. Suzuki, H., Hayashi, K. and Terada, O., Mechanisms of surrounding structure formation in sintered TiC–MO_2C–Ni Alloy. *J. Jpn. Inst. Met.*, 1981, **35**(9), 245–273.
7. Ahn, S. Y. and Kang, S., Formation of core/rim structure in Ti (CN)–WC–Ni cermets via a dissolution and precipitation process. *J. Am. Ceram. Soc.*, 2000, **83**(6), 1489–1494.
8. Ettmayer, P. and Lengauer, W., The story of cermets. *Powder Metall. Int.*, 1989, **21**, 37–38.
9. Jia, K., Fischer, T. E. and Gallois, B., Microsturcture, hardness and toughness of nanostructured and conventional WC–Co composites. *Nanosturctured Mater.*, 1998, **10**(5), 875–891.
10. Seung, I. C., Soon, H. H., Gook, H. H. and Byung, K. K., Mechanical properties of WC–10Co cemented carbides sintered from nanocrystalline spray conversion processed powders. *Int. J. Refract. Met. Hard Mater*, 2001, **19**, 397–403.
11. Liu, N., Xu, Y. D., Li, H., Li, G. H. and Zhang, L. D., Effect of nano-micro TiN addition on the microstructure and mechanical properties of TiC based cermets. *J. Eur. Ceram. Soc.*, 2002, **22**(13), 2409–2414.
12. Jeon, E. T., Joardar, J. and Kang, S., Microstructure and tribo-mechanical properties of ultrafine Ti (CN) cermets. *Int. J. Refract. Met. Hard Mater.*, 2002, **20**, 207–211.
13. Azaroff, L. V. and Buerger, M. J., *The powder method*. McGraw-Hill, New York, 1958.
14. Zackrisson, J. and Andrén, H. O., Effect of carbon content on the microstructure and mechanical properties of (Ti, W, Ta, Mo)(C, N)-(Co, Ni) cermets. *Int. J. Refract. Met. Hard Mater.*, 1999, **17**, 265–273.
15. Lindahl, P., Mainert, T., Jonsson, H. and Andren, H. O., Microstructure and mechanical properties of a (Ti, W, Ta, Mo) (C, N)-(Co, Ni) type cermet. *J. Hard Mater.*, 1993, **4**, 187–204.
16. Zackrisson, J., Thuvander, M., Lindahl, P. and Andren, H. O., Atom probe analysis of carbonitride grains in (Ti, W, Ta, Mo) (C, N) (Co/Ni) cermets with different carbon content. *Appl. Sur. Sci.*, 1996, **94–95**, 351–355.
17. Lindahl, P., Rosen, A. E., Gustafson, P., Rolander, U. and Andren, H. O., Effect of pre-alloyed raw materials on the microstructure of a (Ti, W) (C, N)-Co cermet. *Int. J. Refract. Met. Hard Mater.*, 2000, **18**, 273–279.
18. Ahn, S. Y., Kim, S. and Kang, S., Microstructure of Ti (CN)–WC–NbC–Ni Cermets. *J. Am. Ceram. Soc.*, 2001, **84**(4), 843–849.
19. Yoshimura, H., Sugisawa, T., Nishigaki, K. and Doi, H., Reaction during sintering and the characteristics of TiC–20TiN–15WC–10TaC–9Mo–5.5Ni–11Co cermet. *Int. J. Refract. Met. Hard Mater*, 1983, **12**, 170–174.
20. Penrice, T. W., Some Characteristics of binder phase in cemented carbide. *Int. J. Refract. Met. Hard Mater.*, 1997, **15**, 113–121.
21. Samsonov, G. V. and Vinitskii, I. M., *Handbook of refractory compounds (translated from Russian)*. IFI/Plenum Data Company, NY, USA, 1980.
22. Lindahl, P., Gustafson, P., Rolander, U., Stals, L. and Andrén, H. O., Microstructure of model cermets with high Mo or W content. *Int. J. Refract. Met. Hard Mater.*, 1999, **17**, 411–421.
23. Monteverde, F., Medri, V. and Bellosi, A., Microstructure of hot-pressed Ti (C, N)-based cermets. *J. Eur. Ceram Soc.*, 2002, **22**, 2587–2593.

24. Bellosi, A., Medri, V. and Monteverde, F., Processing and properties of Ti (C, N)–WC-based materials. *J. Am. Ceram. Soc.*, 2001, **84**(11), 2669–2676.
25. *Handbook of Chemistry and Physics* (66th ed.), ed. R.C. Weast. CRC Press Inc., 1986.
26. Mari, D., Bolognini, S., Feusier, G., Cutard, T., Viatte, T. and Benoit, W., TiMoCN based cermets part II. Microstructure and room temperature mechanical properties. *Int. J. Refract. Met. Hard Mater.*, 2003, **21**, 47–53.
27. Zheng, Y. and Xiong, W., Effect of powder particle size on the properties and microstructure of Ti (C, N)-based cermet. *Rare Met.*, 2001, **20**(1), 47–51.
28. Zhang, S., Titanium carbonitride-based cermets: processes and properties. *Mater. Sci. Eng. A*, 1993, **163**, 141–148.
29. Liu, N., Shi, M., Xu, Y. D., You, X. Q., Ren, P. P. and Feng, J. P., Effect of starting powders size on the Al_2O_3–TiC composites. *Int. J. Refract. Met. Hard Mater.*, 2004, **22**, 265–269.